Proceedings of ASME Turbo Expo 2011
GT2011
June 6-10, 2011, Vancouver, British Columbia, Canada

GT2011-46371

INFLUENCE OF SURFACE ROUGHNESS ON THE PROFILE AND END-WALL LOSSES IN LOW PRESSURE TURBINES

Raúl Vázquez [(1)(2)], Diego Torre[(1)], Fernando Partida[(1)], Leyre Armañanzas[(1)] and Antonio Antoranz[(1)]

[(1)] ITP Industria de Turbo Propulsores S.A. Madrid, SPAIN
[(2)] Associated Professor, UPM, Universidad Politécnica de Madrid, SPAIN

ABSTRACT

The influence of surface roughness on the profile and end-wall total pressure losses in Low Pressure Turbines was investigated experimentally in a turbine high-speed rig. The rig consisted of a rotor-stator configuration. Both rows of airfoils are high lift, high aspect ratio and high turning blades that are characteristic of state of the art Low Pressure Turbines.

The stator airfoils (both vanes and platforms) were casted and afterwards they were barreled to improve their surface finish up to 1.73 μm Ra. Then they were assembled in the rig and tested. The stator was traversed upstream and downstream with miniature pneumatic probes to obtain total pressure, flow angle and static pressure flow fields.

Once this test was completed the rig was disassembled and the stator airfoils were polished to achieve a roughness size of 0.72 μm Ra, characteristic of Low Pressure Turbine polished airfoils. Once again, the stators were assembled in the rig and tested to carry out a back-to-back comparison between the two different surface roughnesses.

The total pressure profile and end-wall losses were measured for a wide range of Reynolds numbers, extending from $8x10^4$ to $2.4x10^5$, based on suction surface length (Re_s~1.5 Re_{Cx}) and exit Mach number of 0.61.

Experimental results are presented and compared in terms of area average, radial pitchwise average distributions and exit plane contours of total pressure losses, flow angles and helicity.

The results agree with previous studies of roughness in Turbines, a beneficial effect of surface roughness was found at very low Reynolds numbers, in stagnation pressure losses.

INTRODUCTION

The effects of surface roughness on gas turbine have been studied for over half a century. Some of those studies have been focused on the impact of the degradation of gas turbines with service. Some of them have been explored the effect of the surface roughness on the turbine and compressor performances and some of them have been devoted to heat transfer in turbines. An excellent review of all those publications is documented by J. P. Bons [1]. Actually, the present paper belongs to the second group and therefore the objective of this research is to study the effects of surface roughness in Low Pressure Turbines performance in depth.

As it is well known, roughness influences turbine performance. Roughness effects are dependent on Reynolds number and roughness size. At low Reynolds number, roughness can reduce or eliminate laminar separation bubbles, thus reducing loss, whereas at high Reynolds number, where the boundary layer is turbulent, roughness can increase the boundary layer momentum thickness, thus increasing loss.

Several authors have studied the effect of roughness in profile losses of turbine airfoils, Boyle [2], Hummel [3], Roberts [4], Vera [5], Matsuda [6] and Montis [7] among others. On the contrary, very few have paid attention to the effect of roughness in endwall losses of turbine airfoils as Matsuda [6]. All the previous authors developed their research over linear cascade and none of them selected the material and the manufacturing process used in airfoils of real turbines (casting in Ni-based alloys). Their main findings and results will be reviewed and compared to the results of this paper later.

Low Pressure Turbines for aircraft engines operate in a wide range of Reynolds number, from high altitude (43 kft) to sea level. In this wide range, the Reynolds number based on the suction side length can vary from 10^5 to $5x10^5$, for large turbines. The efficiencies of these turbines are strongly dependent on Reynolds number, thus reducing the efficiency at low Reynolds numbers (high altitude). This efficiency reduction is known as Reynolds Lapse.

The airfoils of these turbines are casted and after a needed surface treatment, reach a characteristic surface roughness around 2.2 μm Ra. Some turbine manufacturers live with that surface roughness, while others for some specific applications apply an additional polishing to reduce the surface roughness to 0.8 μm Ra or even 0.5 μm Ra (superpolished airfoils).

The critical Reynolds number (roughness Reynolds number value corresponding to $k^+=5$) for these turbines is approximately 100. The regime below this threshold is known as “hydraulically smooth” and inside this regime the roughness peaks, are wholly immersed in the laminar sublayer of the turbulent boundary layer ($y^+<5$) and no increase on pressure loss should be expected with increasing roughness [8]. On the contrary, over this limit the regime is called transitional rough or fully rough and the roughness effect on the pressure losses can be relevant.

For a typical axial chord of a large turbine airfoil of 30 mm, the roughness Reynolds number over the critical Reynolds number have been represented in the figure 1 for the two characteristic surface roughness mentioned earlier, 2.2 and 0.5 μm Ra, as function of the operation altitude.

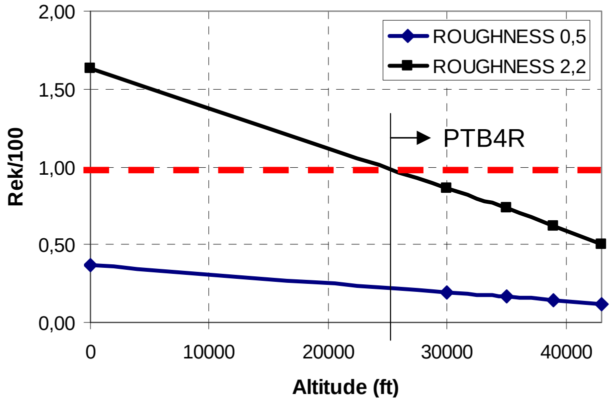

Figure 1, Variation of roughness Reynolds number over critical Reynolds number with altitude.

As it can be seen in figure 1, the working range of superpolished airfoils (roughness 0.5 μm Ra) are well below the critical Reynolds number (red line in figure 1) in the whole operation range and therefore no effects of roughness on pressure losses should be expected. However, this is not the case for rough airfoils (roughness 2.2 μm Ra). Those airfoils operate in the transitional rough zone at low altitude (<25kft) and in hydraulically smooth regime at high altitude (>25kft), see figure 1. So, the rough airfoils should produce more pressure losses (lower efficiency) at sea level than the superpolished airfoils and no significant differences should be expected in cruise conditions between both.

In view of the previous conclusions, the selection of the surface roughness for turbine applications should be straight forward. Turbines that operate at sea level for industrial applications should have polished airfoils. However, turbines for aircraft applications, even more those for large range, should have rough airfoils. Nevertheless, one can find turbines for aircraft applications with polished or even superpolished airfoils. One of the motivations for it, is: the performance of every engine is verified before to be delivered to the customer by means of a pass-off test that is carried out at sea level conditions. Then polishing the airfoils help to achieve the admissible SFC.

Then, the main objective of this research is to validate experimentally that Low Pressure Turbines can operate with rough airfoils at high altitude, let’s say higher than 30 kft, without an efficiency deficit.

In order to achieve this objective a single stage rig (denominated as PTB4R) that is characteristic of modern Low Pressure Turbines was tested. The rig consisted of a rotor-stator configuration (see figure 3). The specimen that is experimentally validated is the stator and the rotor is acting as a wake generator. Hence, the stator is like an unsteady annular cascade with the advantage that the incoming wakes are fully representative because they come from a real rotor. The rig is running at high speed conditions, achieving the cruise Mach number at the stator exit of 0.61.

As mentioned, previous researchs were done in linear cascades and with machining airfoils. Consequently, the work presented in this paper deviates from previous investigations essentially due to the more representative operating conditions (multirow and compressible flow) at which the experiments were carried out and due to the more representative geometry in terms of radial variations and aspect ratio and of course surface roughness in terms of size and topology. On other words, one can state that the Technology Readiness Level (TRL) of the present experiment is higher and therefore the conclusions more reliable.

NOMENCLATURE

Ax	Axial
CTA	Centro de Tecnologías Aeronáuticas
fs	Full Scale
IGV	Inlet Guide Vane
ITP	Industria de Turbo Propulsores S.A.
k_s	Equivalent sand roughness height.
k^+	Equivalent sand roughness in wall units ($k_s u_\tau/\nu$).
KSI	Kinetic Energy Losses ($KSI=1-v^2/v^2_{isentropic}$)
LP	Low Pressure
Ni	Nickel
OD	Outer Diameter
Ra	Arithmetic Average Roughness
Re_s	Reynolds Number (based on exit condition and Suction Surface length/perimeter)
Re_{Cx}	Reynolds Number (based on exit condition and Axial Chord)
Re_k	Roughness Reynolds Number (based on exit condition and equivalent sand roughness, k_s).
SFC	Specific Fuel Consumption
S/S	Suction Side
St	Strouhal Number
TE	Trailing Edge
u_τ	Shear or friction velocity $(\tau/\rho)^{1/2}$.
v	Flow relative velocity
y^+	Distance from the wall in wall units ($y u_\tau/\nu$).

Greek

ν	Kinematic viscosity
ρ	Flow density
τ	Wall stress

EXPERIMENTAL APPARATUS

The experiments were carried out in the transonic wind tunnel at the CTA, in Spain (see figure 2). This is a continuous flow, open circuit, variable density wind tunnel where Reynolds and Mach number can be fixed independently [9]. Two vacuum pumps are used to achieve sub-atmospheric pressures (down to 12 kPa). A two-stages compressor group is used to control the pressure ratio and flow temperature and thus the Mach number of the flow within the circuit. The top mass flow rate achievable is 20 Kg/s. Prior entering the turbine, the air flows through a settling chamber that removes any swirl and axial velocity non-uniformity. Downstream of the settling chamber sits a row of IGV(see figure 3) whose mission is to produce a radial distribution of flow angle and total pressure representative of those found at the inlet of modern LP turbines. Besides, the IGVs may rotate around their stacking axis to achieve the proper off-design inlet flow angle.

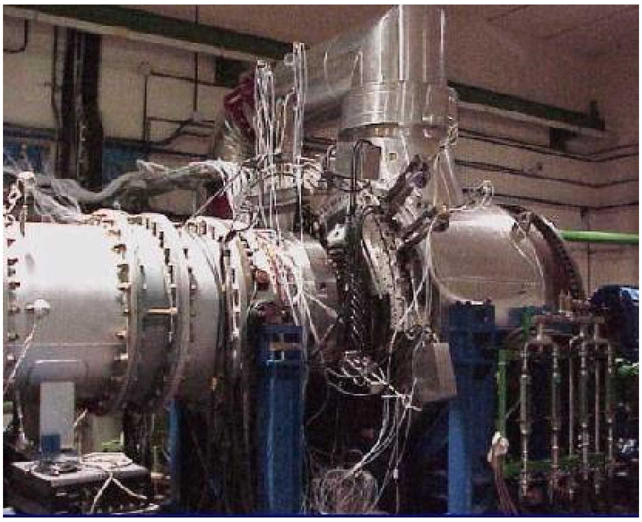

Figure 2, View of the rig installed in the facility.

Additionally, the boundary layer of the outer wall is sucked approximately one chord upstream of the rotor leading edge in such a way that for all the tested conditions the thickness and shape factor are adjusted to similar values than those that exist in turbines operating in engines. In the present study, these were kept almost constant in order to avoid any influence of boundary layer thickness and state in the secondary flow development of the rotor. The inner boundary layer, on the contrary, was considered thin enough to be representative of real turbines and hence it was not tuned.

The stator of this rig consists of 128 high-lift, high turning, aft-loaded, high aspect ratio and radial straight airfoils that are characteristic of front stages of modern LP turbines with a hade angle of 40º. The airfoil profiles are of the solid-thin type (see figure 4). The main parameters of the cascade geometry are given in table 1.

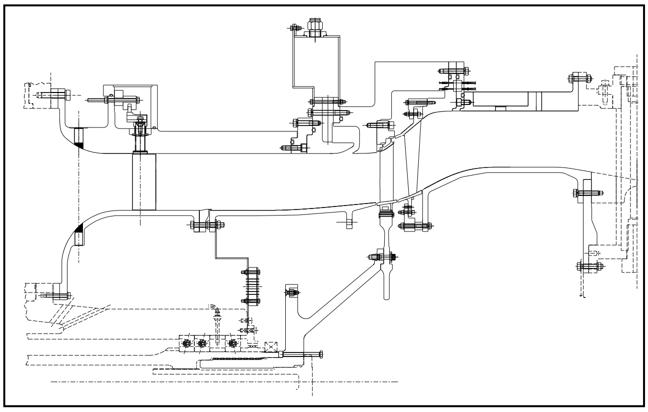

Figure 3, PTB4R rig lay out.

Table 1, Airfoil geometry at mid-span.

Inlet flow angle (deg.)	38.7
Exit flow angle (deg.)	59.4
Velocity ratio	1.7
Pitch/ Ax. Chord	0.8
True Chord/ Ax. Chord	1.07
Suction Side Length/Ax. Chord	1.44
TE thickness/ Ax. Chord	0.015
Lift Coefficient	0.89
Span/Ax. Chord	6.4

The stator airfoils (both vanes and platforms) were casting of a Ni-based alloy characteristic of Low Pressure Turbines. After some needed surface treatment, the expected surface finish should be approximately 2.2 μm Ra. The measured values were slightly lower (average of 1.73 μm Ra) as can be seen in tables 3 and 4. These airfoils will be referred as “roughness 2.2” in the rest of the paper. Then, they were assembled in the rig and tested.

When this test was completed, the rig was disassembled and the stator airfoils were polished. The target roughness size was 0.5 μm Ra, characteristic of LP Turbine superpolished airfoils. However, the measured roughness level were little bit bigger, see tables 3 and 4 (average of 0.72 μm Ra). These stators will be referred in the future as “roughness 0.5”. Once again, the stators were assembled in the rig and tested to carry out a back-to-back comparison between the two different surface roughnesses. The measured arithmetic average roughness of tables 3 and 4 was converted into equivalent sand roughness using the formula $k_s = 8.9Ra$ which was taken from a follow up work of Koch and Smith [10].

This rig, called PTB4R, was part of a group of several rigs, designed and tested by ITP during 2005 and 2006 in the frame of a national research programme. The final goal was to explore the use of distributed roughness as well as single roughness elements as a form of passive flow control.

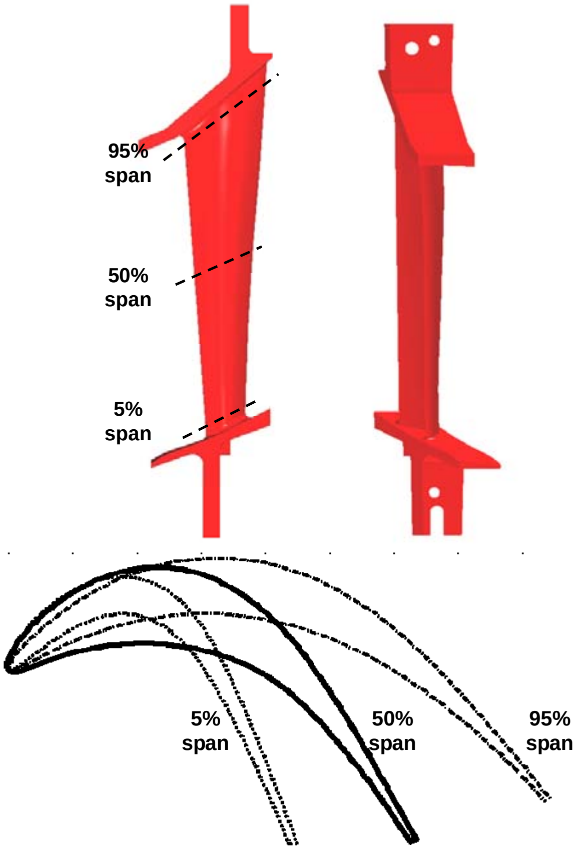

Figure 4, Airfoil geometry: 3D view (top) and 2D view (bottom)

The calculation of total pressure loss across the stator cascade required the flow to be traversed in planes located both approximately 25% axial chord downstream of the rotor TE (referred as inlet plane) and 65% midspan axial chord downstream of the stator TE (referred as exit plane).

For these measurements, miniature fast response five-hole probes were used that were specifically designed and manufactured for these tests. These probes had ø 1.6 mm conical head with 30º and 45ºangle. The size of the holes was 0.3 mm. The probes were L-shape type, with 5.5 mm head length, due to the small blade row gap available. The stem was also 1.6 mm diameter, with 100 mm length, in order to keep the probe blockage lower than 5 %.

The calibration of the probes were performed for a range of Mach numbers from 0.1 to 0.9 and yaw and pitch angles from -60º to 60º, with 2300 points per calibration. The flow angle range could only be achieved, given the cone angle of the probe head, by using a multizone approach as proposed by Johansen et. al [11], and properly facing flow separation issues and probe sensitivity.

Table 2, Airfoil chords, measured on constant span,and Tested Reynolds numbers

	Geometry Details		
	5% Span	50% Span	95% Span
Axial Chord [mm]	14.837	21.688	29.600
Real Chord [mm]	17.570	23.378	30.504
S/S Perimeter [mm]	27.206	37.091	48.186

	Reynolds number based on Perimeter [x10^{-3}]					
5% Span	60.9	81.2	101.5	121.8	142.1	169.1
50% Span	90.0	120.0	150.0	180.0	210.0	250.0
95% Span	101.3	135.1	168.9	202.7	236.4	281.5

	Reynolds number based on Axial Chord [x10^{-3}]					
5% Span	33.2	44.3	55.3	66.4	77.5	92.2
50% Span	52.6	70.2	87.7	105.3	122.8	146.2
95% Span	62.2	83.0	103.7	124.5	145.2	172.9

Table 3, Measured Surface Roughness (Ra) and Equivalent Sandgrain Roughness (k_s) for both airfoil and platforms

	Ra [μm]	ks [μm]
Roughness Case 2.2 μm	1.73	15.40
Roughness Case 0.5 μm	0.72	6.41

Table 4, Measured Ra and Equivalent Sandgrain Roughness (k_s) relative to the Axial Chord

Ra / Axial Chord [x10^5]	5% Span	50% Span	95% Span
Roughness case 2.2 μm	11.7	8.0	5.8
Roughness case 0.5 μm	4.9	3.3	2.4

ks / Axial Chord [x10^5]	5% Span	50% Span	95% Span
Roughness case 2.2 ◊m	103.8	71.0	52.0
Roughness case 0.5 ◊m	43.2	29.6	21.7

Table 5, Range of Experimental Reynolds Numbers based on Ra and Equivalent Sandgrain Roughness (k_s).

Reynolds No. based on Ra [x10^{-3}]	5% Span		50% Span		95% Span	
	Min	Max	Min	Max	Min	Max
Roughness case 2.2 μm	3.9	10.8	4.2	11.7	3.6	10.1
Roughness case 0.5 μm	1.6	4.5	1.8	4.9	1.5	4.2

Reynolds No. based on ks [x10^{-3}]	5% Span		50% Span		95% Span	
	Min	Max	Min	Max	Min	Max
Roughness case 2.2 μm	34.5	95.7	37.4	103.8	32.4	89.9
Roughness case 0.5 μm	14.3	39.8	15.6	43.2	13.5	37.4

Both area traverses upstream and downstream of the stator were extended to the full span and around 2000 points per airfoil channel were employed. In order to reduce the duration of each test, the probe was moved continuously. The velocity of the probe movement was fixed to an enough low value (3.3 m/s traversing velocity) in order to avoid flow disturbance (St ~ 10^{-2}). The overall test time for traversing five flow channels (10^4 mesh points) was around 45 minutes.

An ad-hoc static calibration of the five Endevco pressure transducers was performed before and after the test. During the test the effects of the temperature was compensated externally. Endevco 136 DC signal conditioning systems was used for both the probe pressure excitation and signal conditioning. Data acquisition was carried out through a National Instruments PXI system. The transducer output, excitation intensity, zero shift value, the probe actuator position and the reference pressure, all of them were recorded. The estimated experimental uncertainty for the absolute value of total pressure is expected to be better than 10 Pa (approximately ±2.5% relative uncertainty for the overall value of KSI). However the experiments show a much higher precision for differences of KSI, a repeatability better than 1% can be seen in the results, for instance in figures 6 or 11. That good repeatability allows the comparison between both cascades.

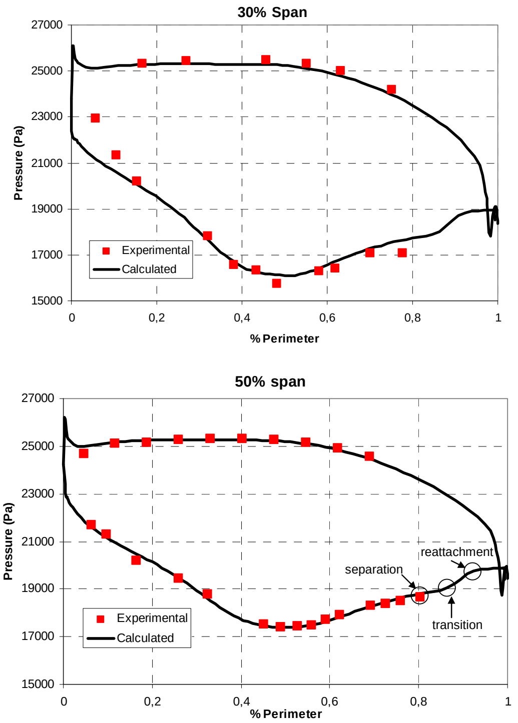

Figure 5, Calculated and measured pressure coefficient over the airfoil surface. Top: 30% span, bottom: 50% span. Re_S = 9x 10^4.

Additionally, static pressure fields on the surface of the stator were measured in five different spanwise locations (see two of them in figure 5). A miniature Pitot tube of 0.2 mm (O.D.) was also used to traverse the upstream inner and outer boundary layers For those tappings the pressure was registered with a "Scanivalve 3018" differential pressure transducer of 35 kPa range and a precision of ± 0.05% fs (approximately 0.18 % of exit dynamic head). Lastly, total temperature was measured using thermocouples (type T) placed upstream and downstream of the cascade.

Vorticity results were calculated from the five-hole probe data following the method proposed by Gregory-Smith et al. [12].

Six different operating conditions corresponding to different Reynolds numbers (see table 2) were investigated, all of them corresponding to a flight altitude higher than 25 kft (see figure 1). Those test cases will be identified in the rest of the paper by the value of the Reynolds number at midspan. In all the cases, the Mach number was fixed to 0.61. Mach and Reynolds numbers are based on the exit velocity and the characteristic length for the Reynolds number is the suction surface length. The corresponding Reynolds numbers in terms of roughness size (Ra and k_s) are also shown in table 5.

RESULTS AND DISCUSSION

A critical description of the experimental results obtained in PTB4R rig is presented in this section. Attention has been focused on revealing the impact of the two surface roughness on the overall, profile and endwall losses.

Variation of measured mixed-out average overall kinetic energy losses with Reynolds number for the two roughness configurations is shown in figure 6. Overall losses were evaluated from the mix-out average quantities at inlet and exit planes. At low Reynolds number it can be seen that losses for the roughness 2.2 set were reduced. For Reynolds number higher than 1.5x10^5, the effect of the roughness on the cascade losses can be considered neutral. The differences between the two sets are very small (<10 Pa), within the experimental uncertainty band. As conclusion, measurements show that roughness is affecting overall losses only at Reynolds numbers under 1.5x10^5.

In the rest of the paper, the KSI has been normalized by the overall KSI value corresponding to the surface roughness of 0.5 μm at the highest Reynolds number (2.4x10^5).

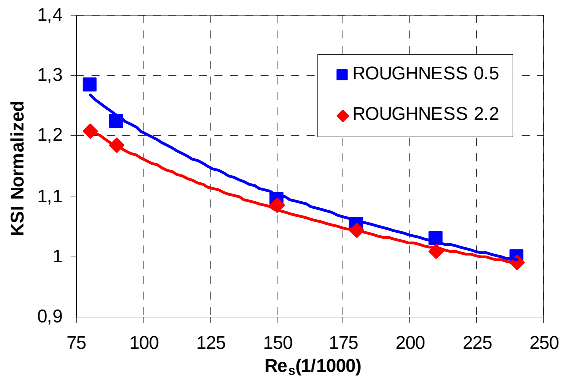

Figure 6, Variation of measured mix-out average KSI with Reynolds number

Figure 7 shows the variation with Reynolds number of the profile losses. Profile losses are evaluated as the pitchwise mixed-out average kinetic energy losses between 45 and 55% of the span. This is done in order to mitigate the effect of non-uniformities in the measurements that could happen at a certain span location. The comparison of profile losses of the two sets leads to similar conclusion to that observed in the overall losses. Profile losses of roughness 2.2 set has been also reduced for Reynolds numbers under $1.5x10^5$, however for higher Reynolds numbers the differences are again negligible. That conclusion agrees with the results of other authors.

All the published data show a trend of increasing roughness effect on airfoil losses with increasing Reynolds number. The increased loss is attributted to both roughness-induced transition and increased turbulent boundary layer momentum losses [1 , 2, 3 and 7]. This effect is not seen in the present results. The maximum roughness Reynolds number that was tested (see Table 5) was not over the critical Reynolds number corresponding to the present experiment. For PTB4R airfoil, this threshold was estimated in ~100 based on numerical calculations This Reynolds number is very close to those obtained by other authors, as Nikuradse [13] and Schilichting [14] as well as Leipold et al. [15] and Bammert [16] for compressor airfoils. Therefore, both roughness configurations were in the "hydraulically smooth" regime for the whole range of tested Reynolds numbers. The roughness peaks, were wholly immersed in the laminar sublayer of the turbulent boundary layer (y^+<5) and no increase on pressure loss should be expected with increasing roughness [8].

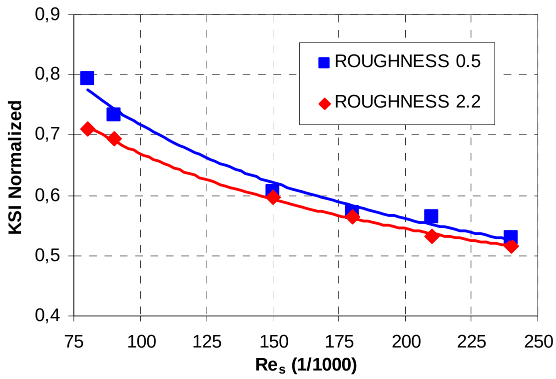

Figure 7, Variation of measured mix-out profile losses with Reynolds number

However, at very low Reynolds numbers, previous works [4,5, 2 and 7] have shown that roughness can also promote transition in separated free shear layers, thus reducing the size of separation bubbles and actually reduce profile losses. This conclusion agree with the results of PTB4R rig (see figure 7). In view of the loading distributions of PTB4R stator at Re_S = $9x10^4$ (figure 5), there is a separation bubble in the suction side preceded by a laminar boundary layer, characteristic of a high lift design. The onset of separation is located around the 80% of the suction side perimeter, the onset of the transition at 90% and the boundary layer reattachment around 96%. Unfortunately, due to the small size of this airfoil, the closer pressure tapping to the trailing edge was located too far from it. Then, the onset of the transition and the reattachment could not be captured by the experimental pressure tappings (see figure 5) and there are not direct experimental evidences that connect the stagnation pressure loss reduction with the size of the separation suction side bubble. No significant differences were found between the rest of the pressure readings for the two tested surface roughness.

Focusing now in the details of the laminar boundary layer upstream of the separation, the k^+ for the surface roughness of 2.2 μm at Re_S = 9 10^4 was approximately 3. This value is far from the critical values proposed by other authors for distributed roughness, as Braslow [17], who suggested a criterion of k^+ >19. Also, the roughness Reynolds number of this laminar boundary layer (~40) is below the critical number (~100) that was obtained from the measurements carried out by Feindt [18]. Therefore, although the size of the roughness in PTB4R do not seem enough big to promote transition, the reduction in the measured losses suggest that those roughness elements can produce additional large amplitude disturbances in the laminar flow that cause an early onset of transition.

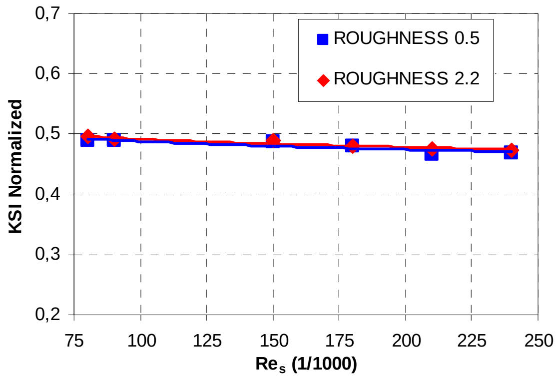

Figure 8, Variation of measured mix-out endwall losses with Reynolds number

The measured reduction in stagnation pressure losses in the lower Reynolds number range was 8%. This benefit proves that the surface roughness can be exploited as a form of passive flow control. From the presented results, the benefit at cruise conditions, in terms of overall efficiency for small and medium turbines can be up to 0.5%. For large turbines, no benefit should be expected in cruise because of the highest airfoil Reynolds numbers. However a considerable reduction (~0.25%) of the Reynolds lapse from 35kft to 43kft could be achievable by increasing roughness.

The previous results show that for the studied airfoils the profile losses are dominating the behaviour of the overall losses. Then, one should not expect a significant impact of the roughness in the endwall losses.

Endwall losses variation with Reynolds number is shown in figure 8. Endwall losses are calculated as the difference between overall and profile losses. For all the tested Reynolds number, endwall losses of both sets are almost identical. This is consistent with figures 6 and 7 showing roughness having similar effect in overall and profile losses. Also, for both sets, endwall losses are not affected by Reynolds number variation.

This insensitivity of endwall losses for low pressure turbines has been already reported by previous works (Vazquez et al. [19] and Hodson and Dominy [20]).

In order to check if the two conclusions obtained for figure 8 are applicable to both endwalls, inner-wall and outer-wall contribution to endwall losses have been separated. Their variation with Reynolds number for the two roughness configurations are shown in figures 9, top and bottom respectively. It can be seen that most of the endwall losses are generated at tip region. Tip endwall losses are higher in the set with roughness 2.2 whereas at inner-wall the opposite trend can be seen. However, the differences between the two sets in both endwalls are very small, and they could be due to the experimental uncertainty. Therefore, to some extent the conclusions applicable to the overall endwall losses derived from the figure 8 can also be applicable to inner and outer wall losses.

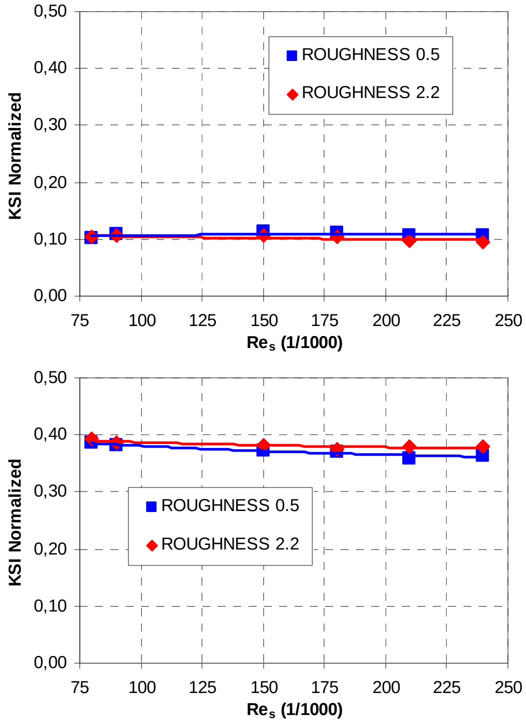

Figure 9, Variation of measured mix-out endwall losses with Reynolds number. Inner-wall (top) and outer-wall (bottom).

Very few authors have explored the influence of roughness on endwall secondary flows in turbines. Matsuda et al. [6] measured the profile and endwall total pressure losses in a large-scale vane cascade with varying degrees of surface polish ($0.8\ 10^{-5}<R_z/c<8.4\ 10^{-4}$). He found a marked rise in endwall losses for the large roughness cases (up to 50%). This conclusion seems to be contradictory to the results of this paper, however important differences exist between both studies that can justify the discrepancies. The two roughness set investigated here are similar to the cases 5 and 7 (C5 and C7) of Matsuda. Nevertheless, Matsuda tested both cases at much higher roughness Reynolds numbers than the maximum Reynolds used in the present study (468 and 1093 versus 43 and 100). The former ones are well above the critical Reynolds number as it can be inferred from the Matsuda's results, being their profile losses strongly affected by the roughness between both configurations (C5 and C7). In those cases where Matsuda kept the roughness Reynolds numbers below the critical value of 100, cases 1 and 2 (C1 and C2), no evidences of roughness impact on overall losses (neither profile nor endwall) were found. Thus, the last statement agrees with the conclusions from PTB4R.

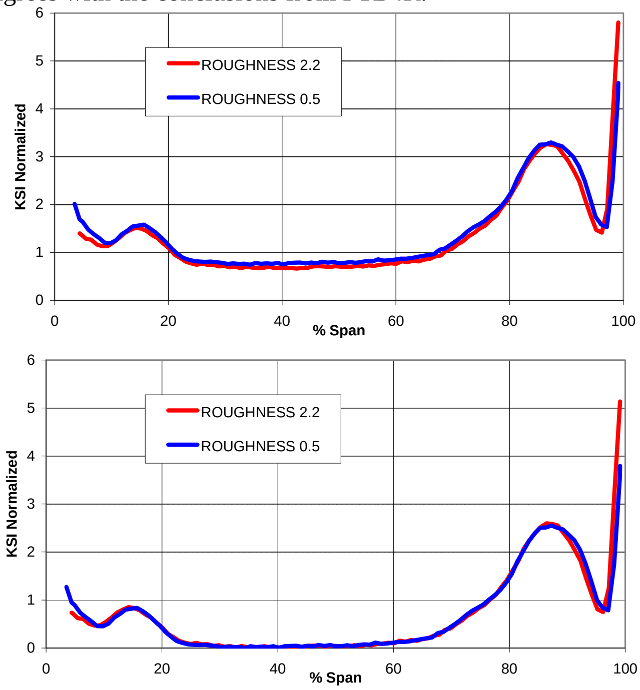

Figure 10, Variation of measured pitchwise mix-out average distribution of kinetic energy losses with roughness at Re_S = 8 x10^4. Overall normalized KSI (top) and net endwall losses (bottom).

In order to know if the small differences found in the inner-wall losses and outer-wall losses between both set of roughness (see figure 9) are real or they are due to the experiment uncertainty, the pitchwise average radial distribution of losses and the contour plots of KSI and helicity at the exit plane are going to be analysed.

Figure 10 (top) shows the measured spanwise distribution of the kinetic energy losses at Reynolds number $8x10^4$. At each span position kinetic energy losses are calculated from the mixed-out average quantities at the exit plane. Inlet variables are taken from the span location in which the mass flow is the same as in the corresponding exit span position. Because of the probe geometry, it was not feasible to traverse the flow located from the inner wall to 4.4 % span and above 99% span. Therefore, spanwise distributions are plotted just between those positions.

Reduction in profiles losses for the roughness 2.2 can be seen in figure 10 top. Also, hub and tip loss cores due to secondary flows can be distinguished. It is noticeable the higher secondary losses at tip region compared to hub region.

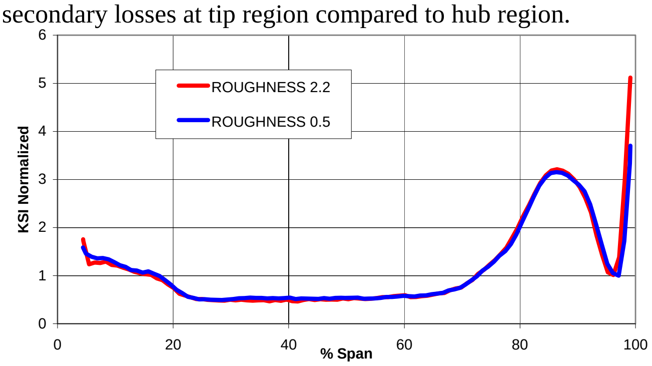

Figure 11, Variation of measured pitchwise mix-out average distribution of kinetic energy losses with roughness at $Re_S = 2.4x10^5$.

The differences in endwall losses are easier to see in figure 10 bottom. This figure reproduces the net endwall losses that are obtained from the overall KSI subtracting the profile losses. It can be seen that secondary loss peak value at tip region is slightly higher for the set with 2.2 μm of roughness. Also in this set, losses in the region from 97% to 99% span, which corresponds with the new endwall boundary layer, are higher. Nevertheless, tip loss core is narrower, which counteracts the above effects and finally leads to similar secondary loss value at tip region, as it has been already seen in figure 9.

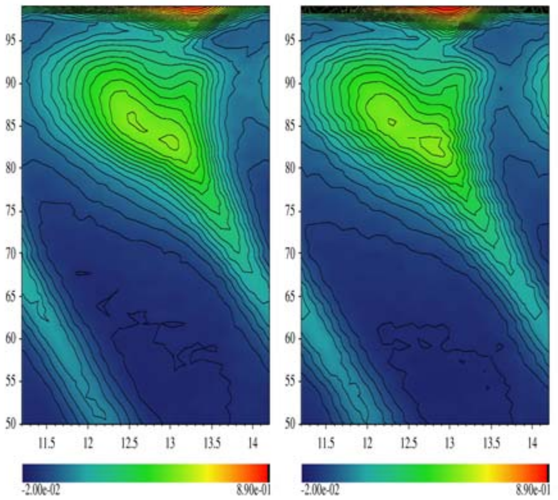

Figure 12, Measured Kinetic Energy Losses contours at exit plane from mid span to 99% of span. $Re_S = 8x10^4$. Roughness 0.5 (left) and roughness 2.2 (right).

Radial distribution of kinetic energy losses at Reynolds $2.4x10^5$ is shown in figure 11. At tip region, the differences between both sets are similar to those observed in figure 10. The loss core in the set with roughness 2.2 is more intense and narrower. In any case, spanwise size of the loss core in roughness 2.2 set has not been as greatly reduced as at Reynolds number $8x10^4$. The losses at new tip endwall boundary layer are still higher for this set. This probably leads to the higher measured tip endwall losses in roughness 2.2 set.

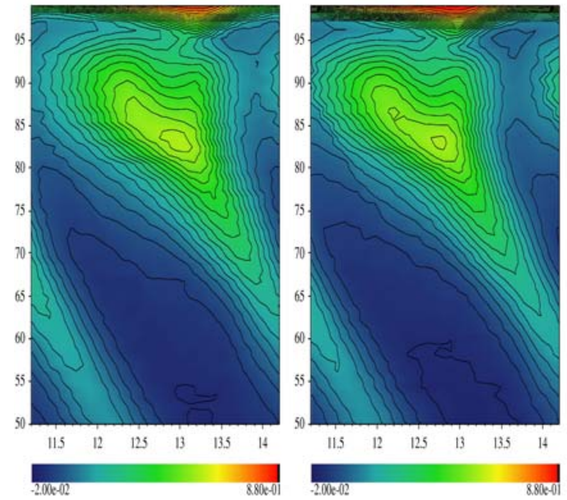

Figure 13, Measured Kinetic Energy Losses contours at exit plane from mid span to 99% of span. $Re_S = 2.4x10^5$. Roughness 0.5 (left) and roughness 2.2 (right).

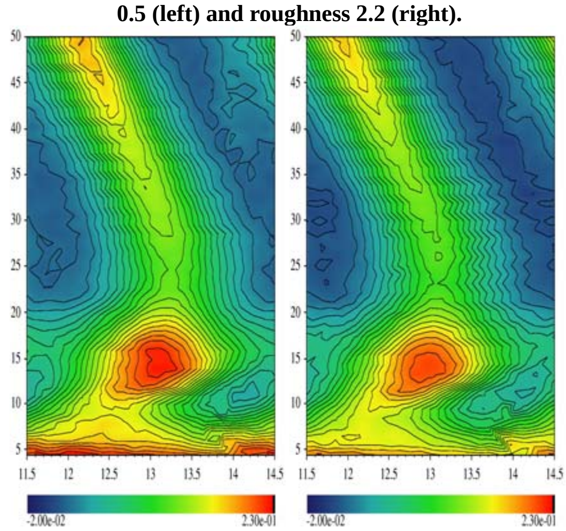

Figure 14, Measured Kinetic Energy Losses contours at exit plane from 4% span to 50% of span. $Re_S = 8x10^4$. Roughness 0.5 (left) and roughness 2.2 (right).

Those features of the outer endwall secondary flows can also be seen in figures 12 and 13. The contour plots of KSI show a slightly more intense red area at the endwall for the largest roughness for both Reynolds number. Regarding the loss core, there are no differences at Reynolds number $2.4x10^5$ however a Reynolds $8x10^4$ the loss core for the largest roughness is marginally smaller.

The increase of endwall losses in the new endwall boundary layer for the largest roughness case was also reported by Matsuda [6]. He found an additional 30% increase of endwall losses for the C7 configuration between a smooth endwall and a rough endwall. Obviously, the increase of losses measured in PTB4R was much lower and it is fair to say that again the roughness Reynolds number tested by Matsuda was well above the critical one, whereas in PTB4R was below that threshold, at least over the airfoil surface.

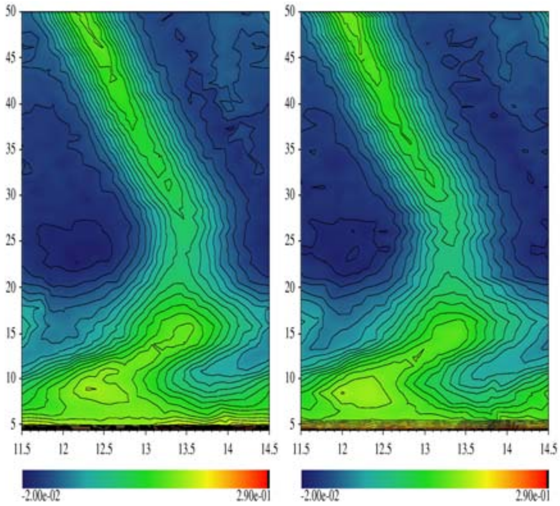

Figure 15, Measured Kinetic Energy Losses contours at exit plane from 4% span to 50% of span. $Re_S = 2.4x10^5$. Roughness 0.5 (left) and roughness 2.2 (right).

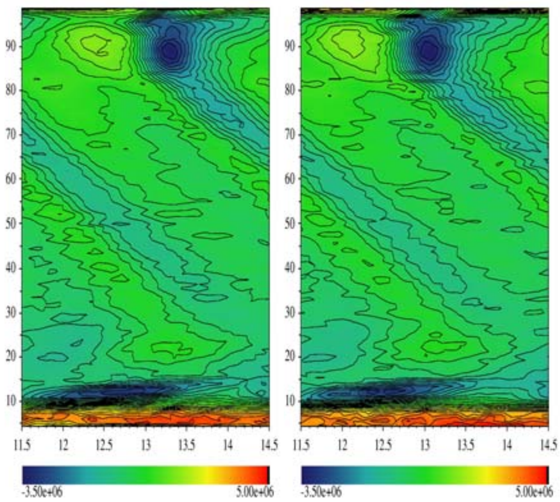

Figure 16, Measured Helicity contours at exit plane from 4% span to 99% of span. $Re_S = 8 x10^4$. Roughness 0.5 (left) and roughness 2.2 (right).

Regarding hub region (see figure 10 bottom), the set with roughness 2.2 has slightly higher losses in the region between 10% and 15% span and lower losses between 10% and 4.4% span, where the passage vortex is located in accordance with the area of positive helicity in figure 16. These opposite effects produce similar hub endwall losses between both roughness configurations at Reynolds $8x10^4$. KSI contours for hub region at Reynolds $8x10^4$ are plotted in figure 14. In both configurations, only one loss core located at 15% span can be seen. The position and size of this loss core is almost the same in the two roughness configurations whereas the strength is lower in the case with roughness 2.2, which is coherent with figure 10 top. Below 10% span, the reduction in losses in the case with roughness 2.2 can be clearly distinguished, in line with figure 10.

Radial distribution of kinetic energy losses at Reynolds $2.4x10^5$ is shown in figure 11. At this Reynolds number, the loss core related with the hub passage vortex is not clearly seen. A marginal increase of losses from 25% span till 4.4% span is seen. In all this entire region, losses of roughness 2.2 set are lower and lead to a lower measured value of hub endwall losses, already observed in figure 9. At this Reynolds number the differences are too marginal and then it is very hard to appreciate them in the KSI contour plots of figure 15.

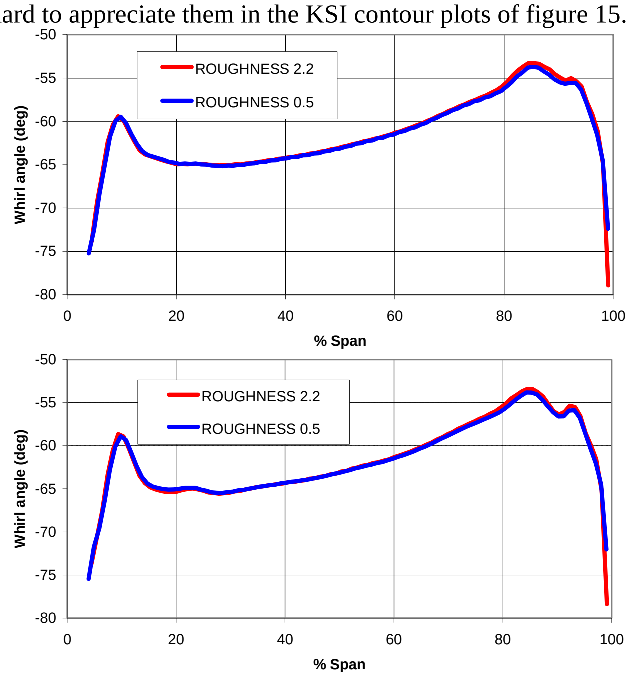

Figure 17, Measured pitchwise mix-out average whirl angle at two Reynolds numbers. $Re_S = 8x10^4$ (top) and $Re_S = 2.4x10^5$ (bottom).

Measured helicity contours at the exit plane are compared at Reynolds $8x10^4$ for completeness in figure 16. As expected from the previous results, the helicity contours confirm that the roughness has not effect on the secondary flows structure. Similar vortices with similar values of helicity can be seen.

Finally, figure 17 shows the spanwise distribution of the pitchwise mixed-out averaged whirl angle for Reynolds number $8x10^4$ and $2.4x10^5$ respectively. It can be seen that for both Reynolds numbers, the whirl angle is little affected by roughness. But some differences can be observed. At tip region, between 80 and 95% span, the set with roughness 2.2 has an underturning 0.5 degrees higher. This might be consistent with the higher strength in the tip loss core observed in figures 10 and 11. Also, overturning is higher in this set, which can be also in line with the higher losses in this region in the set with roughness 2.2. In the other hand, whirl angle at hub secondary flow region is almost the same for the two roughness configurations and for the two Reynolds numbers.

CONCLUSIONS

The effect of surface roughness on Low Pressure Turbines at high altitude operating conditions (over 25 Kft) has been experimentally studied. The same unsteady annular cascade has been characterized with two different surface roughness. First with 2.2 μm Ra and second with 0.5 μm Ra, representative of superpolished airfoils.

The experiment results have proven that the use of rough airfoils in Low Pressure Turbines at high altitude does not introduce additional pressure losses. Otherwise these airfoils can reduce the Reynolds lapse and even for small and medium turbines can improve the efficiency at cruise operating conditions.

This improvement comes from the profile loss reduction and it might be justified by a reduction of the separation suction side bubble. That bubble has a significant contribution to profile loss because of the large adverse pressure gradient that exist in the rear part of the S/S and because of the low operating Reynolds number.

However the endwall losses, the helicity and the exit flow angle are almost not affected by the roughness. There is a small loss increase on the outer end-wall for the rough airfoil, probably due to a thicker new endwall boundary layer.

ACKNOWLEDGMENTS

The authors wish to thank ITP for their support of the project and their permission to publish this paper.

REFERENCES

[1] Bons, J.P., “A Review of Surface Roughness Effects in Gas Turbines,” Journal of Turbomachinery, Vol. 132 pp. 021004-1 to 021004-16.

[2] Boyle, R. J., and Senyitko, R. G., 2003, “Measurements and Predictions of Surface Roughness Effects on Turbine Vane Aerodynamics,” ASME Paper No. GT2003-38580.

[3] Hummel, F., Lotzerich, M., Cardamone, P., and Fottner, L., 2005, “Surface Roughness Effects on Turbine Blade Aerodynamics,” ASME J. Turbomach.,127, pp. 453–461.

[4] Roberts, S. K., and Yaras, M. I., 2004, “Boundary Layer Transition in Separation Bubbles Over Rough Surfaces,” ASME Paper GT2004-53667.

[5] Vera, M., Zhang, X. F., Hodson, H., and Harvey, N., 2007, “Separation and Transition Control on an Aft-Loaded Ultra-High-Lift LP Turbine Blade at Low Reynolds Numbers: High-Speed Validation,” ASME J. Turbomach., 129, pp. 340–347.

[6] Matsuda, H., Otomo, F., Kawagishi, H., Inomata, A., Niizeki, Y., and Sasaki, T., 2006, “Influence of Surface Roughness on Turbine Nozzle Profile Loss and Secondary Loss,” ASME Paper No. GT2006-90828.

[7] Montis, M., Niehuis, R. and Fiala, A., 2010, “Effect of Surface Roughness on Loss Behaviour, Aerodynamic Loading and Boundary Layer Development of a Low-Pressure Gas Turbine Airfoil”, ASME Paper No. GT2010-23317.

[8] Jimenez, J., 2004, “Turbulent Flows Over Rough Walls,” Annual Review Fluid Mechanics 2004.36:173-96.

[9] Vázquez, R., Iturregui, J.J, Arsuaga, M. and Armañanzas, L.,”A New Transonic Test Turbine Facility,” XVI International Symposium on Air Breathing Engines (ISABE) 2003.

[10] Koch, C. C., and Smith, L. H., Jr., 1976, “Loss Sources and Magnitudes in Axial-Flow Compressors,” ASME J. Eng. Power, 98, pp. 411–424.

[11] Johansen, E.J., Rediniotis, O.K., Jones, G., “The Compressible Calibration of Miniature Multi-Hole Probes,” Journal of Fluids Engineering, Vol. 123, pp. 128 –138, March 2001.

[12] Gregory-Smith D.G., Graves C.P., and Walsh J.A., (1988), “Growth of Secondary Losses and Vorticity in an Axial Turbine Cascade.”, Journal of Turbomachinery, 110, 1-8.

[13] Nikuradse, J., 1933, “Laws for Flows in Rough Pipes,” VDI-Forchungsheft 361, Series B, Vol. 4 English translation NACA TM 1292, 1950.

[14] Schlichting, H., 1979, Boundary Layer Theory, 7th ed., McGraw-Hill, New York.

[15] Leipold, R., Boese, M., and Fottner, L., 2000, “The Influence of Technical Surface Roughness Caused by Precision Forging on the Flow Around a Highly Loaded Compressor Cascade,” ASME J. Turbomach., 122, pp. 416–425.

[16] Bammert, K., and Woelk, G. V., 1980, “The Influence of the Blading Surface Roughness on the Aerodynamic Behavior and Characteristics of an Axial Compressor,” ASME J. Eng. Power, 102.

[17] Braslow, A.L., 1960, “Review of the Effect of Distributed Surface Roughness on Boundary-Layer Transition,” AGARD Report No. 254.

[18] Feindt, E. G., 1956, “Untersuchungen uber die Abhangigkeit des Umschlages laminar-turbulent von der Oberflachenrauhigkeit und der Druckverteilung,” Diss. Braunschweig, Jb. 1956 Schiffbautechn. Gessellschaft 50, pp. 180–203.

[19] Vázquez, R., Antoranz, A., Cadrecha, D. and Armañanzas, L., “The influence of Reynolds number, Mach number and Incidence Effects on Loss Production in Low Pressure Turbine Airfoils,” ASME Turbo Expo 2006 (GT2006-91121).

[20] Hodson, H.P. and Dominy, R.G., “The Off-Design Performance of a Low-Pressure Turbine Cascade,” Journal of Turbomachinery, Vol. 109 pp. 201-209.